Fast Prediction of Loadability Margins Using Neural Networks to Approximate Security Boundaries of Power Systems

Xueping Gu
School of Electrical Engineering
North China Electric Power University
Baoding, Hebei Province, 071003, China
(e-mail: xpgu@ncepubd.edu.cn)

Claudio A. Cañizares
Department of Electrical and Computer Engineering
University of Waterloo, Waterloo, ON N2L 3G1, Canada
(e-mail: ccanizar@uwaterloo.ca)

Abstract: Determining loadability margins to various security limits is of great importance for the secure operation of a power system, especially in the current deregulated environment. A novel approach is proposed in this paper for fast prediction of loadability margins of power systems based on neural networks. Static security boundaries, comprised of static voltage stability limits，oscillatory stability limits, and other operating limits, such as generator power output limits, are constructed by means of loading the power system until these security limits are reached from a base operating point along various loading directions. Back-propagation neural networks for different contingencies are trained to approximate the security boundaries. A search algorithm is then employed to predict the loadability margins from any stable operating points along arbitrary loading directions through an iterative technique based on the trained neural networks. The simulation results for the IEEE two-area benchmark system and the IEEE 50-machine test system demonstrate the effectiveness of the proposed method for on-line prediction of loadability margins.

1 Introduction

In the operation of power systems, maintaining the system in a secure operating region is of prime importance to system operators. Typically, loadability margins considering various security limits are the main tools of interest to operators, and hence being able to determine these margins on-line would allow system dispatchers to properly monitor the system.

Power system security involves many limits, i.e. equipment thermal and voltage limits, generation capability limits, voltage stability, oscillatory stability and transient stability limits, which define the system loadability margins [1]. Extensive research work has been conducted on loadability margin determination considering static voltage stability [2]-[8]. The continuation-power-flow method may be the most reliable technique to calculate loadability margins along a given loading direction by tracing the system P-V curves, which may be associated with a saddle-node bifurcation or a limit induced bifurcation [2]. In [3], an interior-point nonlinear optimization method is proposed to obtain a set of optimal loading parameters that maximizes system loadability. On the other hand, a method based on multiple load flow solutions is proposed in [4] to obtain the “minimum” loadability margins. In [5], an energy-function-based approach is proposed to evaluate the loadability margins on a given loading direction. The authors in [6] maximize the loadability margin in a given loading direction through minimizing the reactive power losses near the critical loading point by means of linear programming. In [7], a method for monitoring the maximum permissible loading based on voltage

Xueping Gu worked as a visiting professor in Department of Electrical and Computer Engineering of University of Waterloo from July 2005 to June 2006.
Paper accepted for publication in *IET Generation, Transmission & Distribution*, December 2006.

stability limits is proposed, simplifying the system using Thevenin equivalent circuits for each load bus. The authors in [8] propose a boundary identifier tracing framework using a predictor-corrector technique to evaluate the loadability margins for different control parameter settings and a given loading direction, considering voltage and oscillatory stability.

More recently, some research work has been conducted on the loadability margin evaluation considering oscillatory stability limits, which can be associated with Hopf bifurcations [9]-[10]. In [9], a linear index is proposed for oscillatory instability prediction by computing the minimum singular value of a modified full Jacobian matrix, whereas in [10], the real part of the critical eigenvalue is identified using stochastic subspace identification technique, which is then proposed as an index to predict loadability margins.

Since the 1990s, extensive research work has been carried out on the application of neural networks to power system problems [11]. The neural network is a highly efficient computational tool that could be used for on-line loadability evaluation. Some research work has been devoted to neural network applications to voltage security assessment and monitoring [12]-[16]. Multi-layered feed-forward neural networks have been used for power margin estimation associated with static voltage stability by means of different training criteria and algorithms. The active and reactive powers on load and generation buses are frequently used as the inputs to the multi-layered feed-forward neural networks [12]-[15]; bus voltages and angles are also part of the inputs in some research work [12], [14]; and in [16], the active and reactive power flows of some selected lines are also used as inputs. In [13], active power margins are predicted based on saddle node bifurcation and Hopf bifurcation point detection. In [14], a hybrid neural network consisting of a Kohonen network and a multi-layered feed-forward neural network is proposed, with the Kohonen network as a front-end to cluster input patterns with similar features to improve the generalization ability of the multi-layered feed-forward neural network. The main drawback of these neural-network-based approaches is that they predict the loadability margin for each operating point only for a specific loading direction, which is defined by fixed load distribution coefficients. Some researchers have proposed the use of neural networks for small-signal stability assessment by eigenvalue estimation or stability classification [17]-[19], but these neural networks are not designed for loadability margin prediction.

From the previous discussions, it is clear that the problem of loadability prediction still needs further investigation for on-line applications. In the operation of practical power systems, different loading directions may result in very different loadability margins for the same operating point; hence, loadability margins should be predicted for any loading direction. It would also be advantageous to consider voltage stability, oscillatory stability and other system operating limits, such as generator power output limits, in a unified framework [10], [13]. Therefore, this paper considers these issues to present a novel approach for prediction of loadability margins based on neural networks. The proposed method is based on computing a large number of voltage stability, oscillatory stability limits and other operating limits, which are represented as loading margins for various loading directions from a base operating point, by means of continuation-power-flow and eigenvalue studies. Through approximating the security boundary defined by these limits using a back-propagation neural network, the loadability margins can be quickly predicted from any operating point along arbitrary loading directions. The main features of the proposed approach are that the loading direction for prediction can be arbitrarily given, and that various stability and operating boundaries are considered under the same framework. The numerical results obtained for the IEEE two-area benchmark system and the IEEE 50-machine test system demonstrate the effectiveness of the proposed approach.

2 Construction of the security boundary

2.1 Definitions

A power system can be represented by the following differential and algebraic equations:

$$\begin{aligned} \dot{x} &= f(x, y, p, \lambda) \\ 0 &= g(x, y, p, \lambda) \end{aligned} \tag{1}$$

where x is a vector of the state variables, such as generator speed and torque angles; y is a vector of algebraic variables, such as load terminal voltages; p is a vector of controllable parameters, such as generator terminal voltage settings; and λ is a group of non-controllable parameters, such as active and reactive load powers. When λ changes, the operating conditions change, and hence the system may become insecure.

In the operation of power systems, the system load usually presents different variation patterns. When the system load increases along a specific loading direction, the operating point may reach the system security boundary. Therefore, the loadability margin is defined as the active power load margin from the current operating point to the security boundary.

Let $\lambda = [\lambda_1 \ \lambda_2 \ \dots \ \lambda_n]^T$ in (1) represent a set of load parameters corresponding to load increase rates. In this case, the power system loads change as follows:

$$\begin{aligned} P_i &= P_{i0} + \Delta P_i = (1+\lambda_i) P_{i0} \\ Q_i &= Q_{i0} + \Delta Q_i = (1+\lambda_i) Q_{i0} \end{aligned} \tag{2}$$

where P_{i0} and Q_{i0} are the active and reactive powers at the ith (i=1,2,…,n) load bus for the base operating condition. The parameters λ_i can then be represented as:

$$\begin{aligned} &\lambda_i = \alpha d_i \\ \Rightarrow &\lambda = \alpha [d_1 \ d_2 \dots d_i \dots d_n]^T \end{aligned} \tag{3}$$

where $\alpha \geq 0$ is a scalar factor typically referred to as the loading factor. The parameters $d_1, d_2, \dots, d_n$ define a loading direction as follows:

$$D = [d_1 \ d_2 \dots d_i \dots d_n]^T \tag{4}$$

where $0 \leq d_i \leq 1$, with the following equation being satisfied:

$$\sum_{i=1}^{n} d_i = 1 \tag{5}$$

Once the loading direction is defined, the system load can be increased to a security boundary by increasing the loading factor α. Observe from the definition of D that the parameters d_i (i = 1, 2,…, n) are greater than or equal to zero, i.e. all the loading directions are restricted to the first quadrant in the d-parameter space.

In steady-state operation, the security region is typically defined by various types of boundaries, i.e. static voltage stability, oscillatory stability and other operating limits. The concept of defining a static security boundary and its associated secure region is illustrated in the λ-parameter space for a 2-dimesional example in Fig.1. In this figure, λ_1 and λ_2 are the load increase rates for loads 1 and 2; by increasing the loading factor from the base point (0, 0) along a certain direction D_r, one of the 3 security boundaries may be reached. The loadability margin from the base point to the security boundary at the ith load can be given by

$$\Delta P_i = \alpha_r^c d_{ir} P_{i0} = \lambda_{ir}^c P_{i0}$$
$$\Delta Q_i = \alpha_r^c d_{ir} Q_{i0} = \lambda_{ir}^c Q_{i0} \quad (6)$$

where α_r^c is the critical loading factor, and λ_{ir}^c is the critical load increase rate for the *i*th load, in the direction D_r.

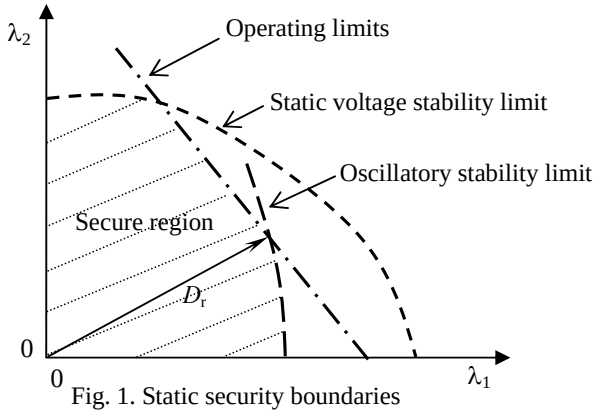

Fig. 1. Static security boundaries

After all the critical loading factors at different loading directions are obtained, a "unified" security boundary can be determined in the λ-parameter space. A boundary point *k* is determined by $\lambda^k = [\lambda_1^k \ \lambda_2^k]^T$, where

$$\lambda_1^k = \alpha_k^c d_{1\underline{0k}}$$
$$\lambda_2^k = \alpha_k^c d_{2\underline{0k}} \quad (7)$$

and α_k^c is the critical loading factor from the base point to the boundary point *k* along $D_{\underline{0k}} = [d_{1\underline{0k}} \ d_{2\underline{0k}}]^T$. By "rotating" the $D_{\underline{0k}}$ from the pure λ_1 direction [1, 0] to the pure λ_2 direction [0, 1] at a given rate, one can obtain a group of boundary points defined by α_k^c and $D_{\underline{0k}}$ (*k*=1,2,…, *m*). These boundary points can be used to train a back-propagation neural network to approximate the security boundary using $D_{\underline{0k}}$ as inputs, and $\alpha_k^c \ \forall k$ as the expected outputs.

2.2 Computational process

To obtain the boundary points to build the training and test samples of the neural network, continuation-power-flow and eigenvalue analysis techniques are combined to calculate critical loading factors along different loading directions, and assuming certain generation dispatch (in this paper, generators were assumed to be loaded in proportion to their available power, i.e. the difference between the generators' capacity and their power levels at the base loading conditions). After defining the loading directions, the saddle node bifurcation and limit induced bifurcation boundary points are first obtained by continuation-power-flow analysis, and the Hopf bifurcation boundary points are then calculated by eigenvalue analysis in an iterative manner using a dichotomy method applied to the voltage stability boundary obtained with the continuation-power-flow. In the process of finding the saddle node bifurcation, limit induced bifurcation and Hopf bifurcation boundary points, the generator power limits are monitored; if the generation powers reach their limits, the boundary points are then defined by a generator output limit boundary. The computational process can be summarized as follows:

1) Define all the loading directions with an even distribution in the *d*-parameter space.
2) Carry out power flow and eigenvalue analysis at the base operating point.

3) Calculate the saddle node bifurcation and limit induced bifurcation boundary points along all the selected loading directions using a continuation-power-flow program.
4) Calculate the Hopf bifurcation boundary points by eigenvalue-analysis and the generator output limit points within the voltage stability limits obtained in item 3.
5) The 3 types of boundaries are used to define a unified security boundary representing the maximum allowed loading factors.

It is important to mention that an N-1 contingency criteria should be used to obtain this unified security boundary. If no contingencies are considered, a stability rather than a security boundary is obtained through this process.

In this study, UWPFLOW [20] was used to obtain the voltage stability boundary, and PST [21] was used to obtain the oscillatory stability boundary. To avoid inconsistent power flow solutions between UWPFLOW and PST for operating points close to the voltage stability boundary, the power-flow solution from UWPFLOW was used as the input for PST, since this program is a more robust tool to obtain solutions near voltage collapse points.

2.3 Determination of loading directions

To construct a continuous boundary, the loading direction points should have an even distribution and reasonable density in the *d*-parameter space to guarantee that no big holes occur on the boundary surface. The loading direction points in the *d*-parameter space are represented by d_i (i=1,2,…,n), and they should cover the whole scope of $0 \le d_i \le 1$ to get a complete boundary. From the definition, the loading direction points in the *d*-parameter space must satisfy (5); this means that the loading direction points lie on a hyperplane confined by the n axes of the *d*-parameters, and that this hyperplane intersects with the axis d_i at the point $d_i = 1$, for $d_j = 0\ \forall\ j \neq i$.

To get an even distribution of the loading direction points in a multi-dimensional *d*-parameter space, the interval [0 1] on each axis is divided into n_t sections; n_t+1 cutting points that include the two end points 0 and 1 on each axis can then be obtained. All the possible combinations of the cutting points that satisfy (5) are found for all axes by a depth-first search technique [22].

3 Prediction of loadability margins using neural networks

After obtaining the security boundary, a back-propagation neural network can be trained to approximate it for fast prediction of loadability margins, since this neural network can be used for nonlinear mapping and approximation of complex functions. Previous studies show that a 3-layered back-propagation neural network can approximate any nonlinear function with finite discontinuities [23], thus a typical 3-layered back-propagation neural network, with n input neurons and one output neuron, is assumed to be powerful enough to approximate the security boundary in this study.

The inputs of the neural network are the vector entries $D = [d_1\ d_2 \ldots d_i \ldots d_n]^{\mathrm{T}}$, and the output is the maximum loading factor α^c for the selected loading direction; these pairs of inputs and output are used for training. The biases applied to the hidden neurons are defined by $B_1=[b_{11}\ b_{12}\ \ldots\ b_{1N}]^{\mathrm{T}}$, and the bias applied to the output neuron is defined by $B_2=[b_{21}]$. The activation function of the hidden neurons is defined as $f(x) = 2/(1+\mathrm{e}^{-2x}) - 1$ and the output function is defined as $f(x) = 1/(1+\mathrm{e}^{-x})$ [23]. The input neurons are used only to distribute the input data to the hidden neurons, and no activation function is applied to them. The mean-square-error function was used as the training criterion, and the number of hidden neurons N, which varies according to the test system and its topology, was chosen empirically through trial and error.

3.1 Neural network training and test

All the boundary points for neural network training to approximate the security boundary can be obtained by the

method given in Section 2. After obtaining all the boundary points, the associated loading factors are all normalized to values from 0 to 1. All the input-output pairs for all the loading directions are grouped into a sample set for neural network training. After training, the neural network can be used to predict the loading factors from the base point on any loading directions.

The testing samples for the trained neural network were obtained in the *d*-parameter space by choosing m_t loading direction points based on randomly generated *d* values. The security boundary computational process described in Section 2.2 is then used to determine the accuracy of the neural network predictions.

3.2 Prediction of loadability margins from arbitrary operating points

After training the back-propagation neural network, the loadability margins from the given base operating point along any loading directions can be quickly predicted. However, the aim is to predict the loadability margins from any operating point along any loading directions, which would be more useful in power system operation applications. The computational procedure to accomplish this is described below.

The basic principle to determine the loadability margin based on the neural network prediction is illustrated by a 2-dimensional example in Fig. 2. In the λ-parameter space shown in this figure, the point *j* is an arbitrary operating point defined by $\lambda^j = [\lambda_1^j \ \lambda_2^j]^T$, and it approaches the boundary point defined by $\lambda^k = [\lambda_1^k \ \lambda_2^k]^T$ along the $D_{\underline{jk}}$. Suppose that the loading factor from *j* to *k* is α_{jk}, the boundary point λ^k can then be obtained by

$$[\lambda_1^k \ \lambda_2^k]^T = [\lambda_1^j \ \lambda_2^j]^T + \alpha_{jk} D_{\underline{jk}} \tag{8}$$

The loading direction from the base point to the point *k* is then defined as

$$D_{\underline{0k}} = [\lambda_1^k \ \lambda_2^k]^T / (\lambda_1^k + \lambda_2^k) \tag{9}$$

Hence, the loading factor α_{0k} from the base operating point to the point *k* can be predicted by the trained neural network, and the following equation should be satisfied at the point *k*:

$$\alpha_{0k} D_{\underline{0k}} = \lambda^k \tag{10}$$

The point *k* is obtained using the following iterative method: The operating point is first moved from *j* to *h* in Fig. 2 by a loading factor α_{jh} along the given $D_{\underline{jk}}$; therefore, the operating point *h* can be defined by

$$[\lambda_1^h \ \lambda_2^h]^T = [\lambda_1^j \ \lambda_2^j]^T + \alpha_{jh} D_{\underline{jk}} \tag{11}$$

Based at the point $\lambda^h = [\lambda_1^h \ \lambda_2^h]^T$, the $D_{\underline{0h}}$ can be computed using (9), and the neural network can be used to predict the loading factor α_{0h}. If $\alpha_{0h} D_{\underline{0h}} = \lambda^h$, the point *h* is at the boundary point *k*; if $\|\lambda^h\| < \alpha_{0h} \|D_{\underline{0h}}\|$, the loading factor α_{jh} should be increased further; and if $\|\lambda^h\| > \alpha_{0h} \times \|D_{\underline{0h}}\|$, the loading factor α_{jh} should be decreased. After some iterations with appropriate step adjustments, the point *h* will be close to the boundary point *k* within certain tolerance. When the boundary point *k* is obtained by computing the loading factor α_{jk}, the MW loadability margin from the point *j* to *k* can be easily computed as follows:

$$\Delta P_{mar} = \sum_{i=1}^{n} (\lambda_i^k - \lambda_i^j) P_{i0} \tag{12}$$

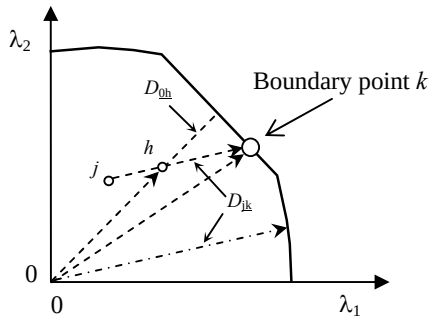

Fig. 2. Basic principle to find the loadability margin based on neural network prediction

In this paper, the problem of estimating "intermediate" critical loading factors is treated as a problem of finding the root of a nonlinear equation, as follows: By defining the following functions:

$$\lambda^h = f_1(\alpha_{jh}) \tag{13}$$

$$D_{\underline{0h}} = f_2(\alpha_{jh}) \tag{14}$$

$$\alpha_{0h} = f_{NN}(D_{\underline{0h}}) \tag{15}$$

where f_1 is directly obtained from (11), f_2 is obtained from (9), and f_{NN} is a mapping function representing the neural network, a function f_{e} can be defined as:

$$f_e(\alpha_{jh}) = \left\| f_1(\alpha_{jh}) \right\| - \left\| f_2(\alpha_{jh}) f_{NN}(f_2(\alpha_{jh})) \right\| \tag{16}$$

This function can be used to estimate the desired critical loading factor by solving the nonlinear equation:

$$f_e(\alpha_{jh}) = 0 \tag{17}$$

The root α_{jh}^* of (17) must lie in the interval [0, $\alpha_{\max}$], where $\alpha_{\max}$ is the maximum loading factor for all loading directions; notice that 0 and $\alpha_{\max}$ are two "extreme" roots of (17). The following algorithm, which is based on the bisection method [24], is used here to obtain the desired root of (17):

a) Set the initial operating point defined by λ^{j}, and give the loading direction $D_{\underline{ik}}$.
b) Let x_1=0, x_2=$K\alpha_{\max}$, where a K value between 1.05 and 1.20 is used to account for the possible prediction errors of the neural network.
c) Let $\alpha_{jh} = (x_1 + x_2)/2$, and compute f_1 in (13).
d) Compute f_2 in (14).
e) Determine f_{NN} using the neural network.
f) Compute f_{e} in (16)
g) If $|f_{\mathrm{e}}| < \xi$, where ξ stands for the convergence tolerance, $\alpha_{jh}^* = \alpha_{jh}$, and stop.

h) If $f_e > 0$, let $x_2 = \alpha_{jh}$; if $f_e < 0$, let $x_1 = \alpha_{jh}$, and repeat the procedure from literal c.

4 Numerical results and discussions

4.1 IEEE Two-area benchmark system

The IEEE two-area benchmark system shown in Fig. 3 is employed here to demonstrate the proposed approach: The generators are modeled using detailed subtransient models, and simple excitation system and speed governor models are used at all generators. A power system stabilizer is installed on the generator G4 to damp possible low frequency oscillations. There are two load buses, namely, Bus 7 (Load 2) and Bus 9 (Load 1), and their load powers at the base condition are 9+j1.0 pu and 17+j1.0 pu, respectively, for a 100MVA base. The active power generation limit is 9.5 pu for each of the generators.

Following classical security analysis methods, voltage stability limits associated with saddle node bifurcations and limit induced bifurcations were determined with the help of PV curves, constructed using a continuation-power-flow program and assuming constant-power load models and constant power factors. Oscillatory stability limits associated with Hopf bifurcations were computed based on eigenvalue studies, where the loads were modeled as 50% constant impedance and 50% constant current.

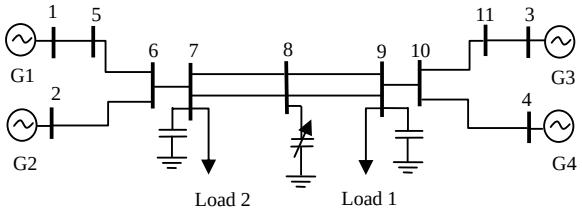

Fig. 3. IEEE two-area benchmark system

4.1.1 Security boundaries

For the normal topology and a Line 8-9 outage, 41 loading directions with an even distribution are defined to construct the unified security boundaries illustrated in Fig. 4 for the two topologies. The parameters λ_1 and λ_2 define the load increase rates of Load 1 and Load 2, respectively.

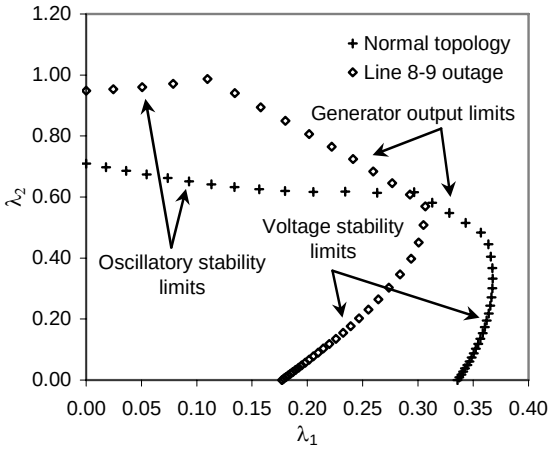

Fig. 4. Security boundaries for the two-area benchmark system

4.1.2 Neural network training and test

Two back-propagation neural networks in the Matlab-based neural network tools are employed to approximate the

security boundaries for the two topologies. Each of the neural networks used has 2 input nodes for the loading direction parameters and 1 output node for the maximum loading factor. From training, the "optimal" number of the hidden nodes chosen is 8.

The 41 boundary points in each of the two topologies are used as the training samples to train the two neural networks separately. The difference between the predicted loading factor value by the neural network and the actual one of a case is defined as the prediction error. The prediction error value divided by the actual loading factor value of the same case is defined as a percentage prediction error. The prediction errors and the percentage prediction errors with the maximum absolute values are 0.001 and 0.12% for the normal topology, and -0.0028 and -0.32% for the Line 8-9 outage, respectively. All the prediction error values for the 41 loading directions are given in Table 1 for the two topologies.

Table 1: Prediction error values from the training samples for the two-area system

loading directions	Normal topology	Line 8-9 outage	*loading directions*	Normal topology	Line 8-9 outage
1	0.00045	-0.00059	21	0.00020	0.00036
2	-0.00040	-0.00166	22	-0.00010	0.00170
3	0.00000	-0.00066	23	-0.00042	0.00082
4	0.00039	-0.00205	24	0.00030	0.00108
5	-0.00028	0.00148	25	0.00018	0.00093
6	0.00057	-0.00151	26	-0.00052	-0.00010
7	0.00001	0.00122	27	-0.00018	-0.00096
8	0.00045	-0.00282	28	-0.00012	0.00224
9	0.00100	-0.00117	29	-0.00085	0.00151
10	0.00038	0.00127	30	-0.00073	-0.00011
11	0.00013	-0.00078	31	-0.00021	-0.00026
12	-0.00022	0.00048	32	0.00003	-0.00011
13	0.00017	-0.00004	33	0.00000	0.00041
14	0.00002	-0.00021	34	0.00014	-0.00038
15	-0.00017	0.00003	35	-0.00008	-0.00013
16	-0.00005	0.00019	36	-0.00014	0.00014
17	0.00012	0.00014	37	0.00009	0.00017
18	0.00009	-0.00004	38	0.00015	0.00007
19	-0.00002	-0.00028	39	-0.00002	-0.00013
20	-0.00017	-0.00013	40	-0.00013	-0.00023
			41	-0.00006	0.00006

To test the ability of the trained neural networks to predict the loadability margins for other cases, 40 new loading directions are randomly created to build test sample sets for each topology. The prediction errors and the percentage prediction errors with the maximum absolute values are -0.0058 and -0.63% for the normal topology, and 0.0027 and 0.33% for the Line 8-9 outage, respectively. The prediction error values for the 40 loading directions are given in Table 2 for the two topologies. From Tables 1 and 2, observe that the back-propagation neural networks can approximate the security boundaries with very high precision, as the prediction error values for the training and test samples are very small.

Table 2: Prediction error values from test samples for the two-area system

loading directions	Normal topology	Line 8-9 outage	*loading directions*	Normal topology	Line 8-9 outage
1	-0.00002	0.00027	21	-0.00581	0.00232
2	-0.00024	-0.00001	22	0.00003	0.00017
3	0.00023	0.00083	23	0.00038	-0.00074
4	-0.00004	0.00016	24	-0.00095	0.00247
5	-0.00032	-0.00055	25	-0.00003	-0.00015
6	-0.00011	0.00149	26	0.00004	0.00016
7	0.00029	0.00097	27	0.00038	-0.00136
8	-0.00053	0.00093	28	-0.00092	0.00271
9	-0.00026	0.00053	29	0.00006	-0.00036
10	0.00010	-0.00075	30	-0.00063	-0.00013
11	0.00002	0.00023	31	-0.00033	0.00047
12	-0.00016	0.00144	32	-0.00020	-0.00010
13	-0.00020	-0.00011	33	-0.00013	-0.00005
14	-0.00035	0.00015	34	-0.00022	-0.00007
15	0.00012	-0.00109	35	-0.00002	0.00018
16	0.00001	0.00020	36	0.00010	-0.00036
17	0.00093	-0.00164	37	-0.00554	0.00234
18	-0.00018	0.00019	38	-0.00018	-0.00025
19	-0.00028	0.00053	39	-0.00018	-0.00003
20	-0.00038	-0.00219	40	-0.00006	-0.00107

4.1.3 Prediction from any operating point

The trained neural networks are then used to predict the loadability margins from any stable operating point along arbitrary loading directions. Three operating points $[0.05\ 0.4]^T$, $[0.1\ 0.2]^T$ and $[0.15\ 0.3]^T$ are selected as the initial operating points, and for each selected point, 5 random loading directions are chosen, for a total of 15 test cases.

The loading factors for all the 15 cases are calculated under the normal topology and for the Line 8-9 outage. The prediction results for both topologies are given by Table 3 and Table 4, respectively; these results show that the prediction of the loading factors is very accurate. The prediction errors and the percentage prediction errors with the maximum absolute values are only 0.0014 and 0.2973% for the normal topology, and 0.0042 and 0.5326% for the Line 8-9 outage.

Table 3: Prediction results of loadability margins for the normal topology

Operating points	loading directions		α values by analysis	α values predicted	Prediction error values	Percentage prediction error values (%)
	d_1	d_2				
0.05, 0.40	0.6712	0.3288	0.4211	0.4206	-0.0004	-0.1034
	0.6738	0.3262	0.4202	0.4199	-0.0003	-0.0662
	0.2915	0.7085	0.3235	0.3236	0.0000	0.0104
	0.3578	0.6422	0.3440	0.3434	-0.0006	-0.1731
	0.4494	0.5506	0.3935	0.3945	0.0010	0.2602
0.10, 0.20	0.3678	0.6322	0.5897	0.5895	-0.0002	-0.0264
	0.0212	0.9788	0.4532	0.4536	0.0004	0.0860
	0.4526	0.5474	0.5505	0.5516	0.0012	0.2143
	0.3720	0.6280	0.5876	0.5873	-0.0004	-0.0620
	0.1981	0.8019	0.5195	0.5199	0.0004	0.0796
0.15, 0.30	0.0476	0.9524	0.3387	0.3383	-0.0004	-0.1148
	0.4442	0.5558	0.4176	0.4174	-0.0002	-0.0448
	0.3367	0.6633	0.4553	0.4567	0.0014	0.2973
	0.1523	0.8477	0.3731	0.3737	0.0006	0.1640
	0.9801	0.0199	0.2218	0.2217	-0.0001	-0.0375

Table 4: Prediction results of loadability margins for the Line 8-9 outage

Operating points	loading directions		α values by analysis	α values predicted	Prediction error values	Percentage prediction error values (%)
	d_1	d_2				
0.05, 0.40	0.6712	0.3288	0.3809	0.3825	0.0017	0.4346
	0.6738	0.3262	0.3793	0.3809	0.0016	0.4198
	0.2915	0.7085	0.5490	0.5501	0.0010	0.1909
	0.3578	0.6422	0.5207	0.5196	-0.0011	-0.2186
	0.4494	0.5506	0.4843	0.4842	-0.0001	-0.0180
0.10, 0.20	0.3678	0.6322	0.5611	0.5623	0.0012	0.2089
	0.0212	0.9788	0.7916	0.7958	0.0042	0.5326
	0.4526	0.5474	0.4410	0.4403	-0.0007	-0.1609
	0.3720	0.6280	0.5545	0.5568	0.0022	0.4057
	0.1981	0.8019	0.6738	0.6727	-0.0011	-0.1674
0.15, 0.30	0.0476	0.9524	0.5826	0.5832	0.0006	0.1075
	0.4442	0.5558	0.3467	0.3466	0.0000	-0.0027
	0.3367	0.6633	0.4425	0.4433	0.0009	0.1961
	0.1523	0.8477	0.5274	0.5264	-0.0010	-0.1810
	0.9801	0.0199	0.1261	0.1261	0.0000	0.0067

4.2 IEEE 50-Machine Test System

To test the effectiveness of the proposed approach in a more realistic environment, the IEEE 50-machine test system [9] is employed to test the proposed loadability margin prediction technique. Basically, the same numbering of buses and generators as those used in [9] is used here as well. Generators 1 to 6 are modeled using subtransient models, and the rest are represented using classical models. A simple excitation system model is used for Generators 1 to 6, and 3 power system stabilizers are installed on Generators 1 to 3 to damp possible low frequency oscillations.

As in the case of the two-area benchmark system and following classical security analysis methods, voltage stability limits were determined with the help of PV curves and assuming constant-power load models and constant power factors, whereas oscillatory stability limits were determined through eigenvalue analyses using constant-impedance load

models.

There are a total of 64 load buses in the system. All the load buses, except Bus 137, are used to simulate load changes, since the maximum loading factor for Bus 137 is very small (about 0.02). The 63 load buses are divided into three groups for load monitoring: Group 1 has 11 load buses, with a total load power of 159089+j42274 MVA; Group 2 has 17 load buses, with a total load power of 86048+j23386 MVA; and all the rest of the load buses are gathered into a third group (Group 3), with a total load power of 5311+j10431 MVA. The loads in each of these 3 groups participate in the loading process with the same participating factor, which means that the load monitoring is carried out in a 3-area λ–parameter space defined by λ_1, λ_2 and λ_3 for Group 1, Group 2 and Group 3, respectively.

4.2.1 Security boundaries

The security boundaries for the normal topology and a Line 67-125 outage are calculated using the proposed procedures. A total of 631 loading directions are defined with an even distribution in a 3-dimensional *d*-parameter space. The security boundaries are comprised of voltage stability points and oscillatory stability points, since no generator output limit points were encountered. Before normalization, the maximum loading factor is 1.0412 and the minimum is 0.2822 among all the loading directions for the normal topology, and 1.0433 and 0.2819 for the Line 67-125 outage. The security boundary for the normal topology is illustrated in Fig.5; observe that the security boundary is a continuous "complex" surface, with the loading factor changing significantly in different loading directions.

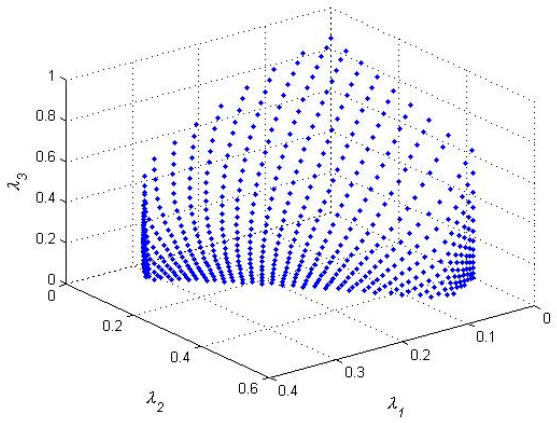

Fig. 5. Security boundary for the normal topology of the 50-machine test system

4.2.2 Neural network training and test

A Matlab-based back-propagation neural network with 3 input nodes and 25 hidden nodes is trained to approximate the security boundary with the 631 training samples for the normal topology; the prediction error and the percentage prediction error with the maximum absolute values for all the training directions are 0.0183 and 2.04%, respectively. A back-propagation neural network with 3 input nodes and 30 hidden nodes is trained to approximate the security boundary for the Line 67-125 outage; the prediction error and the percentage prediction error with the maximum absolute values are 0.0112 and 1.49%, respectively. The prediction error values for all the training samples under the two topologies are depicted in Fig. 6(a)-(b); observe that the approximating errors for the training samples are fairly small, since most of the error values are between -0.005 and 0.005.

To demonstrate the ability of the trained neural networks to predict loadability for a variety of test cases, a total of 200 loading directions are randomly created to test the neural networks for the two topologies. The prediction errors and the percentage prediction errors with the maximum absolute values are 0.0225 and 2.37% for the normal topology, and -0.0167 and -2.22% for the Line 67-125 outage, respectively. The prediction error values for all the test samples for the two topologies are plotted in Fig.6(c)-(d). Notice that the error values for the test samples are slightly larger than that for the training samples, but are still reasonably small; most of test cases have the prediction error values between -0.01

and 0.01. This shows the effectiveness of the trained neural networks for loadability prediction from the base operating point along any loading directions.

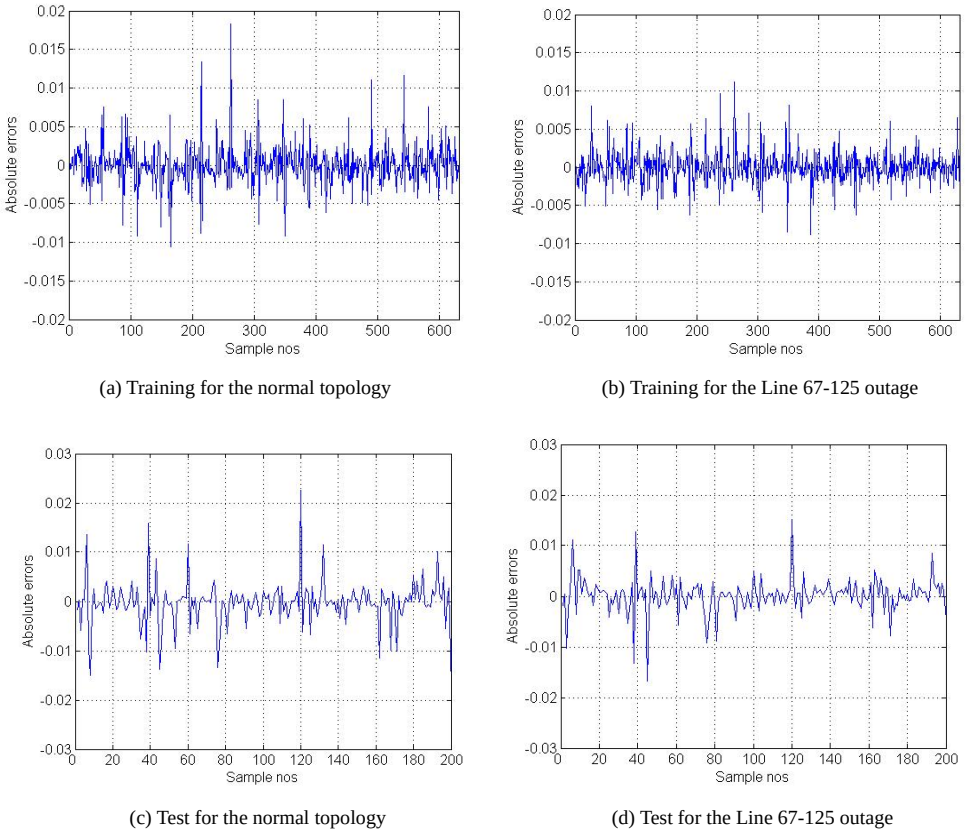

(a) Training for the normal topology

(b) Training for the Line 67-125 outage

(c) Test for the normal topology

(d) Test for the Line 67-125 outage

Fig. 6. Prediction error values from the training and test samples for the 50-machine test system

4.2.3 Prediction from any operating point

The trained neural networks are then tested to predict the loading factors from any operating points along arbitrary loading directions. Five stable operating points, namely, $[0.05\ 0.1\ 0.09]^T$, $[0.08\ 0.15\ 0.08]^T$, $[0.1\ 0.08\ 0.05]^T$, $[0.12\ 0.05\ 0.1]^T$ and $[0.13\ 0.07\ 0.15]^T$, are arbitrarily selected for testing, and 20 loading directions are randomly generated for each operating point, for a total of 100 cases for each of the two topologies. The prediction errors and the percentage prediction errors with the maximum absolute values are 0.0116 and -2.08% for the normal topology, and -0.0101 and 2.14% for the Line 67-125 outage, respectively. The average absolute values of the prediction errors and the percentage prediction errors from all the 100 cases are 0.0018 and 0.55% for the normal topology, and 0.0017 and 0.44% for the Line 67-125 outage, respectively. The obtained prediction results can be considered accurate for the 50-machine test system.

4.3 Practical applications

From the simulation results of the two test systems, the effectiveness of the proposed approach for loadability margin prediction is demonstrated. Hence, using the proposed approach, the loadability margins can be quickly predicted at any operating points along any loading directions. To demonstrate the practical application of the proposed technique, the two-area system is used here as an example. Thus, suppose that the operating point and the loading direction are changed based on the loading pattern shown in Fig. 7. Let the base point represent the night minimum load, and assume that the operating point moves continuously from point 0 back to 0 during the day as illustrated in Fig. 7. The security margins in MW at different operating points can then be easily predicted using a back-propagation neural network

through the day, as depicted in Fig. 8. The “jump” in the margin for an operating point is due to changes in the loading direction.

Using the proposed approach, the security margins at different operating points can be closely monitored. Thus, notice in Fig. 8, that when the system reaches the loading conditions associated with the point 3, the system enters a “warning” region, since the power margin is less than 10% of the total base load (2600MW). If a Line 8-9 outage occurs at point 3, the operating point will fall into an “emergency” region where the power margin is less than 4% of the total base load. Hence, the proposed approach can be a helpful tool for power system operators to make dispatching decisions on-line.

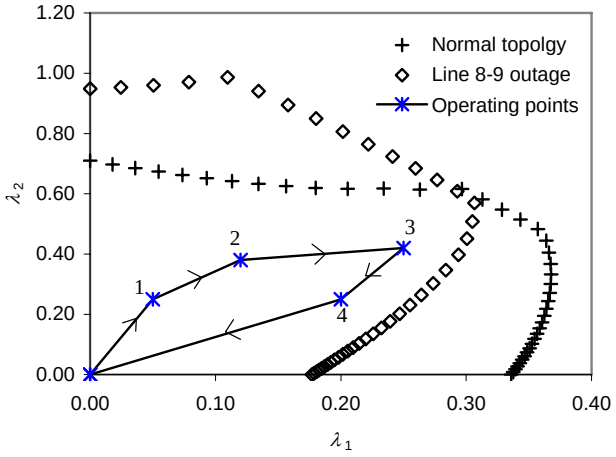

Fig. 7. Operating points during system operation

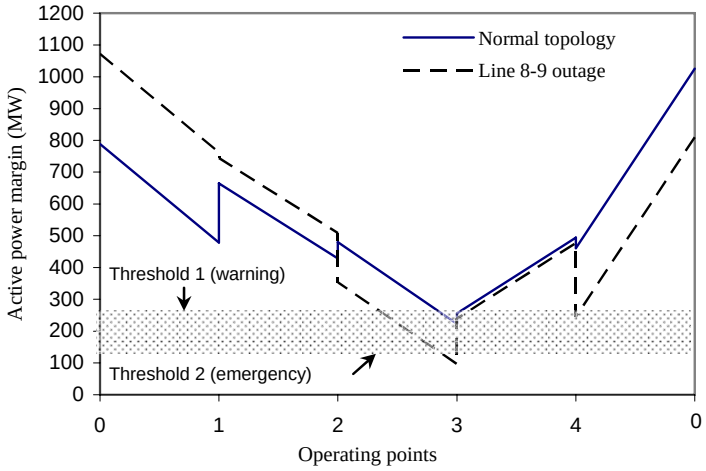

Fig. 8. Security margins represented by the allowed active power increases

In this paper, the loading directions cover the whole scope of the first quadrant of the *d*-parameter space. However, it should be noted that the proposed method can be easily adapted to a more practical case where the loading space may be a restricted cone inside the positive quadrant, by simply narrowing the scope of d_i values (i = 1, 2,…, n) from [0, 1] to [a_i , b_i], where $0 \le a_i, b_i \le 1$ and $a_i < b_i$.

It is also important to highlight the fact that, in practical power systems, there is a large number of load buses; however, it is impractical and also unnecessary to monitor each of the loads individually, since load buses are typically

grouped into zones/areas for the purpose of system security monitoring. Thus, transmission system capacities, which have been classically used to define power system security, are only determined for "key" transmission corridors between well predefined interchange areas. For example, in the case of Ontario, these security limits are typically defined for the main transmission lines interconnecting about 8 zones: Michigan, NY, Quebec, Manitoba, Eastern, South-Western and Northern Ontario, plus the Greater Toronto Area. Therefore, the dimension of the *d*-parameter space in the proposed technique, which is directly associated with these predefined interchange areas, should be a manageable number (e.g. around 10 in most systems), considering that the training of the proposed neural network is done off-line and not on-line.

5 Conclusions

An effective approach to predict loadability margins considering static voltage stability, oscillatory stability and operating limits is proposed based on neural networks. By appropriately selecting a group of loading directions, a back-propagation neural network can be trained to accurately approximate the security boundary to predict loadability margins from a base operating point, and for any other operating point within that boundary. It is shown in this paper, that a properly trained back-propagation neural network can readily be used to quickly monitor the loadability margins during the daily operation of a practical power system.

6. Acknowledgements

Xueping Gu worked as a visiting professor in University of Waterloo from July 2005 to June 2006, under financial support from the China Scholarship Council. The work in the paper was supported in part by a grant from National Natural Science Foundation of China (50577017).

7. References

[1] Balu, N., et,al.: 'On-line power system security analysis', *Proc. IEEE*, 1992, 80, (2), pp. 262-280

[2] Cañizares, C. A., and Alvarado, F. L.: 'Point of collapse and continuation methods for large AC/DC systems', *IEEE Trans. Power Syst.*, 1993, 8, (1), pp. 1-8

[3] Irisarri, G. D., Wang, X., Tong J., and Mokhtari, S.: 'Maximum loadability of power systems using interior point non-linear optimization method', *IEEE Trans. Power Syst.*, 1997, 12, (1), pp.162-172

[4] Yorino, N., Harada, S., and Cheng, H.: 'A method to approximate a closet loadability limit using multiple load flow solutions', *IEEE Trans. Power Syst.*, 1997, 12, (1), pp. 424-429

[5] Klump, R. P., and Overbye, T. J.: 'Assessment of transmission system loadability', *IEEE Trans. Power Syst.*, 1997, 12, (1), pp. 416-423

[6] Tare, R.S., and Bijwe, P.R.: 'Look-ahead approach to power system loadability enhancement', *IEE Proc. – Gener. Transm. Distrib.*, 1997, 144, (4), pp. 357-362

[7] Haque, M. H.: 'Online Monitoring of maximum permissible loading of a power system within voltage stability limits', *IEE Proc. – Gener. Transm. Distrib.*, 2003, 150, (1), pp. 107-112

[8] Zhou, Y., and Ajjarapu, V.: 'A fast algorithm for identification and tracing of voltage and oscillatory stability margin boundaries', *Proc. IEEE*, 2005, 93, (5), pp. 934-946

[9] Cañizares, C. A., Mithulananthan, N., Milano, F., and Reeve, J.: 'Linear Performance Indices to Predict oscillatory Stability Problems', *IEEE Trans. Power Syst.*, 2004, 19, (2), pp. 1104–1114

[10] Ghasemi, H., Cañizares, C., and Moshref, A.: 'Oscillatory stability limit prediction using stochastic subspace identification', *IEEE Trans. Power Syst.*, 2006, 21, (2), pp. 736–745

[11] Haque, M.T., and Kashtiban, A.M.: 'Application of neural networks in power systems – a review', *Transactions on Engineering, Computing and Technology*, 2005, 6, pp. 53-57

[12] Scala, M. L., Trovato, M., and Torelli, F.: 'A neural network-based method for voltage security monitoring', *IEEE Trans. Power Syst.*, 1996, 11, (3), pp. 1332-1341

[13] Popvic, D., Kukolj D., and Kulic, F.: 'Monitoring and assessment of voltage stability margins using artificial neural networks with a reduced

input set', *IEE Proc. – Gener. Transm. Distrib.*, 1998, 145, (4), pp. 355-362

[14] Wan, H.B. and Song, Y.H.: 'Hybrid supervised and unsupervised neural network approach to voltage stability analysis', *Electric Power Systems Research*, 1998, 47, (2), pp.115-122

[15] Srivastava, L., Singh, S.N., and Sharma, J.: 'Estimation of loadability margin using parallel self-organizing hierarchical neural network', *Computers and Electrical Engineering*, 2000, 26, (2), pp. 151-167

[16] Chakrabarti, S., and Jeyasurya, B.: 'On-line voltage stability monitoring using artificial neural network'. Proc. *2004 Large Engineering Systems Conference on Power Engineering*, Westin Nova Scotian, Canada, July 2004, pp. 71-75

[17] Mori, H., Tamaru, Y., and Tsuzhki, S.: 'An artificial neural-net based technique for power system dynamic stability with the Kohonen model', *IEEE Trans. Power Syst.*, 1992, 7, (2), pp. 856-864

[18] Hsu, Y.Y., Chen, C.R., and Su, C.C.: 'Analysis of electromechanical modes using an artificial neural network', *IEE Proc. – Gener. Transm. Distrib.*, 1994, 141, (3), pp. 198-204

[19] Teeuwsen, S.P., Erlich, I., and El-Sharkawi, M.A.: 'Small-signal stability assessment based on advanced neural network methods', *Proc. 2003 IEEE Power Engineering Society General Meeting*, vol. 4, July 2003, pp. 2349-2354

[20] Cañizares, C. A., Faur, Z. T., and Alvarado, F. L.: '*UWPFLOW'*, [On-line] Available: http://thunderbox.uwaterloo.ca/%7Eclaudio/software/pflow.htm

[21] *'Power System Toolbox (PST) Version 2.0: Dynamic Tutorial and Functions'* , (Cherry Tree Scientific Software, 2002)

[22] Luger, G. F.: '*Artificial intelligence – structures and strategies for complex problem solving'*, (New York: Addison Wesley, 2005, 5th ed.)

[23] Demuth, H., and Beale, M.: '*Neural Network Toolbox for Use with Matlab-User's Guide (Version 3.0)'*, (The MathWorks Inc., 1998)

[24] '*Numerical Recipes – Books On-Line*', [On-line] Available: http://www.numerical-recipes.com/nronline_switcher.html, (Numerical Recipes Software)